Supporting Information

Penn et al. 10.1073/pnas.1515105113

SI Materials and Methods

MEA. MEAs of 60 electrodes with a diameter of 30 μm and a spacing of 200 μM (MultiChannelSystems) were prepared by autoclaving and oxygen plasma discharge treatment (Fig. S9). The plasma cleaner (PDC-32G-2; Harrick Plasma) was first purged by oxygen flow with the MEAs inside for 20 min and then operated at the high-power setting for 3 min. Plasma cleaning was followed by overnight application at room temperature of poly-L-lysine (P4707; Sigma) diluted 1:5 in borate buffer. After three rinses with double-distilled water (DDW), the MEAs were left overnight in the incubator with plating medium [5% (vol/vol) FCS; Gibco] and 5% (vol/vol) heat-inactivated horse serum (HIHS; Gibco) in Earle's MEM (Gibco) enriched with 0.6% glucose, 1% Glutamax (Invitrogen), 0.02 mg/mL gentamicin, and 0.1% B-27 supplement. After 4 DIV, 30% of the medium was replaced by final medium [10% (vol/vol) HIHS in Earle's MEM enriched with 0.6% glucose, 1% Glutamax, and 0.02 mg/mL gentamicin]. At 8 DIV, the MEAs were transferred to the final medium, after which one-third of the medium was replenished at intervals of 3 d for 1 wk, followed by 2-d intervals after that time.

Culture Preparation. Rat hippocampal neurons from 19-d-old embryos were used. All procedures were approved by the Weizmann Institute's Animal Care and Use Committee. Following the method of Segal and Manor (39), dissection was carried out in ice-cold L-15 medium enriched with glucose (0.6%) and gentamicin (0.02 mg/mL; Sigma–Aldrich). The hippocampus was dissociated first by enzymatic and then by mechanical trituration. As in previous work (29), neurons were seeded into 3 mm of medium at a typical initial density of 3,000–4,000 neurons per square millimeter, with survival rates that lead to a typical final density of 800 neurons per square millimeter (Fig. S9*A*). Measurements were almost always carried out on 14–17 DIVs (one measurement was on 19 DIV) in a chamber placed on a thermally regulated plate held at 38 °C by water flowing through it. Each culture was measured over one experiment that typically lasted 8–9 h.

Serum-Free Media. We experimented with several different fluid media for the measurement, and found that media containing horse serum led to less regular activity than the serum-free media (Fig. S5). Horse serum (Biological Industries) is collected from a donor herd and tested for its ability to support the growth of Sp2/O-Ag14 (murine myeloma) cells in control medium containing the test lot of serum. Horse serum (different from what is used to develop vaccines) is often used as a component in the growth medium of neuronal cultures. In particular, previous reports on bursting network activity of neural cultures have used it at times in maintaining their cultures even while measuring the activity, particularly over long periods. The ingredients of the horse serum are variable, because it is obtained from an animal, and are not regulated. We use HIHS in which proteins are deactivated by the heat treatment. We present the data with horse serum as an "uncontrolled" environment, where the ionic concentrations and other factors are not well known. This behavior is in stark contrast to the "controlled" medium that we use, in which all of the components are well known and the concentrations of all of the different ions are precisely determined. We have seen that adding the antibiotic gentamicin to the measurement medium affects the stability, so one interesting possibility is that traces of antibiotics that may be present in the horse serum affect the activity.

We therefore conducted the measurements in a controlled medium: DDW containing 5.3 mM potassium, 144 mM sodium, 155 mM chloride, 0.81 mM magnesium, 39 mM glucose, 16 mM sucrose, 10 mM Hepes, and 10 mM Glutamax, but with no serum. Potassium and calcium concentrations were varied according to the experimental protocol described in the main text. Neuronal activity usually equilibrated within several minutes of the transfer to calcium-free medium, which was the first condition that experiments began with as a standard. The calcium-free condition also usually served as a final control at the end of each experimental run, ensuring that the culture had not deteriorated significantly during the experiment. Changes in membrane potential due to ionic content were calculated using the Goldman–Hodgkin–Katz equation with our ionic concentrations (www.physiologyweb.com/calculators/ghk_equation_calculator.html).

Electrophysiology. The electrical signals were amplified 1,200-fold and then low-pass-filtered with a 3-kHz cutoff (MEA1060 amplifier; MultiChannelSystems) and sampled at 13 kHz, using a general-purpose data acquisition board (PCI-6071E; National Instruments). Data were acquired and processed using MATLAB (The MathWorks). The condition for spike detection was that the absolute value of the sampled signal exceeds an amplitude threshold for duration of at least 0.2 ms. The threshold was set at the higher of either 15 μV or sixfold the rms of the signal. Only one dominant form of spike was taken per electrode, eliminating the need for spike sorting and ensuring a clear signature for every electrode. The resulting spike waveforms are shown in Fig. S9*B*, and we verified by spike sorting that in a large portion of the electrodes, typically 90%, the spike shapes were consistent with a single source. The remaining 10% did not give a clear separation into two spikes but could not be assigned unambiguously to one cluster. We can safely conclude that there is only one neuron measured for each of the electrodes we measured, which is confirmed by the fact that no electrode gave consequent spikes that were separated by less than 2 ms and, rarely, less than 5 ms apart. We thus equate an electrode with a single neuron, and use the terms "neuron" and "electrode" interchangeably.

Patch Clamp. Hippocampal cultures at 14 DIV were transferred to a recording chamber placed on the stage of an inverted Olympus IX70 microscope and washed with a serum-free controlled medium. Neurons were recorded with patch pipettes containing 136 mM K-gluconate, 19 mM KCl, 5 mM NaCl, 10 mM Hepes, 0.1 mM EGTA, 0.3 mM Na-GTP, 1 mM Mg-ATP, and 5 mM phosphocreatine (pH 7.2) with a resistance in the range of 5–8 MΩ. Signals were amplified with a MultiClamp 700B instrument and recorded with a pClamp10 (Axon Instruments). Data were analyzed offline using MATLAB.

Calcium Imaging at 1 mM Ca^{2+}. Neuronal cultures (*SI Materials and Methods*, *Culture Preparation*), grown on 13-mm glass coverslips, were preincubated for 1 h in serum-free media containing 1 mM Ca^{2+} and Fluo-4 calcium indicator (Molecular Probes) and placed in a chamber with fresh serum-free media. The chamber was mounted on a Zeiss inverted microscope with a 10× objective. Imaging was obtained using a CCD camera (SensiCam) with a 20-Hz sampling rate and at room temperature. Data were analyzed using MATLAB.

Analysis. The neuronal firing rate is given by the number of spikes or APs measured in a given electrode per bin of 20 ms. The mean firing rate was calculated for each electrode as the total number of spikes measured in a corresponding time interval divided by the time interval (in seconds). Electrodes were deemed active and

retained for further analysis if the mean firing rate during the measurement was above 0.01 Hz.

Oscillations were identified from the FFT of the firing rate, which was calculated by dividing the total interval into segments of 60 s and then averaging over the interval. A neuron was classified as an oscillator if the largest peak in the FFT was 2 SDs larger than the background of the FFT and its full width at two-thirds maximum was 0.15 Hz or less. Fig. S8*A* shows the stability of five representative oscillators, recorded simultaneously over time periods of 6,700 s (*Left*) or 100 s (*Right*) and plotted along with their spectrograms. Fig. S8*B* shows the distribution function of the IBIs for 14 representative neurons, whereas Fig. S8*C* shows the distribution function of the CVs of the IBIs obtained for 235 neurons. The average CV was 0.28.

Summing over all APs in all of the electrodes in bins of 20 ms gives the network activity as a function of time. A network burst is defined to have occurred if 1 s of complete quiescence in all active electrodes was followed by over 60% electrodes that fired within one 20-ms bin. A burst continues until the occurrence of another second of complete silence in the network (Fig. 1 *A* and *B*). The abrupt onset characterizing these global bursts is a well-documented feature of strongly connected neuronal networks (29–31). The burst rate (different from the firing rate) was calculated as the total number of detected network bursts divided by the corresponding time interval (in seconds). The frequency of the network bursts was calculated by the peak in the FFT of the network activity, similar to the single neuron oscillation criterion.

IBIs were measured from the end of one burst until the beginning of the next one. For the fluorescence and patch-clamp data, the end of the burst was harder to evaluate; thus, we also present for comparison the interval between the first spike of one burst and the first spike of the next burst, which are easy to identify. These intervals differ because the length of the burst may vary, as indeed happens at the higher calcium values (1 and 1.5 mM calcium). Significantly, we found that the CV of both distributions was small, indicative of a well-defined period.

Synchrony was examined by looking at the cross-correlation of all of the electrodes with each other, measured for segments of 60 s, which are then averaged over the duration of the experimental condition. The time lag at which this averaged cross-correlation peaks for each pair of electrodes was extracted. When single neurons share a common oscillation frequency, this time lag reflects the mean phase shift between the pair of oscillators. As the synchronization increases, the neuronal spikes bunch into smaller and smaller time intervals and the peaks in the correlation converge to a correspondingly shorter interval around zero-lag. This convergence is shown in Fig. 3*C*. The average over the absolute value of these time lags represents this bunching of the neurons and serves as a quantitative measure of network synchrony. The absolute value needs to be taken, because in Fig. 3*C*, both values for the cross-correlation of two electrodes are given, where one value is the negative of the other. In principle, synchrony can be quantified by this time lag, and one may think of synchrony as the inverse of the time lag in appropriately normalized units, although we do not use this definition in the current work.

Upon increase of the connectivity, correlation emerges in the network and the lags decrease from values on the order of seconds to tens of milliseconds. For the fast-rising bursts, which are characteristic of a strongly connected network (above 1 mM $[Ca^{2+}]_o$), the averaged time lag drops to less than 20 ms (Fig. 3C, *Bottom*). We define this condition as equivalent to zero-lag synchrony.

A tricky point is that if the network is not bursting, as is the case for 0 mM Ca (Fig. 3*C*, *Top*), then a spurious peak can appear simply because the single neuron frequencies are widely distributed and neurons with short periods will have cross-correlations with peaks closer to zero-lag. However, this peak will be very shallow and very broad, on the order of the inverse of the mean frequency. To demonstrate that the phase shift between the neurons is fixed, and thus the order of firing of the neurons within the burst is fixed, the electrodes have been ordered in Fig. 3*C* according to the mean lag with all of the other electrodes.

Recruitment time is related to synchrony, and was defined by the time that passed from the firing of the first spike in the burst until 80% of the neurons that participated in the burst had fired their first spike.

Pharmacology. Synaptic blockers were applied by bath application to block AMPA, NMDA, and GABA receptors, using their respective antagonists: 6-cyano-7-nitroquinoxaline-2,3-dione (10–20 μM), of 2-amino-5 phosphonovaleric acid (50 μM), and bicuculline (40 μM). The calcium chelator EGTA was used at 3 mM in two experiments under the zero calcium condition as a control verifying that no additional effects appeared. Barium was added in the form of $BaCl_2$ at concentrations varying from 2 μM to 3 mM. Riluzole (R116-25MG; Sigma) was administered at 0.3–10 μM to block the persistent sodium current $I_{Na}P$.

SI Discussion

A possible alternative mechanism for creating synchronous neuronal oscillation is electrical coupling (EC) by gap junctions (GJs). This coupling has been suggested as a synchronizing mechanism in emergent high-frequency (200 Hz) oscillations (27), although the action of the specific GJ blocker used there is controversial (28). We observed in our cross-correlation results at 0 mM Ca^{2+} that all pairs of neurons were uncorrelated; thus, if independent and separate synchronizing networks of neighbors are acting, then they must be very small and localized around each electrode. Given the scarcity of GJs in cultures, the EC scenario for synchronization thus seems highly improbable. Another possible scenario is a linkage of glial cells to the neurons that creates a separate frequency at each neuron, but we have found no evidence either for or against such a mechanism.

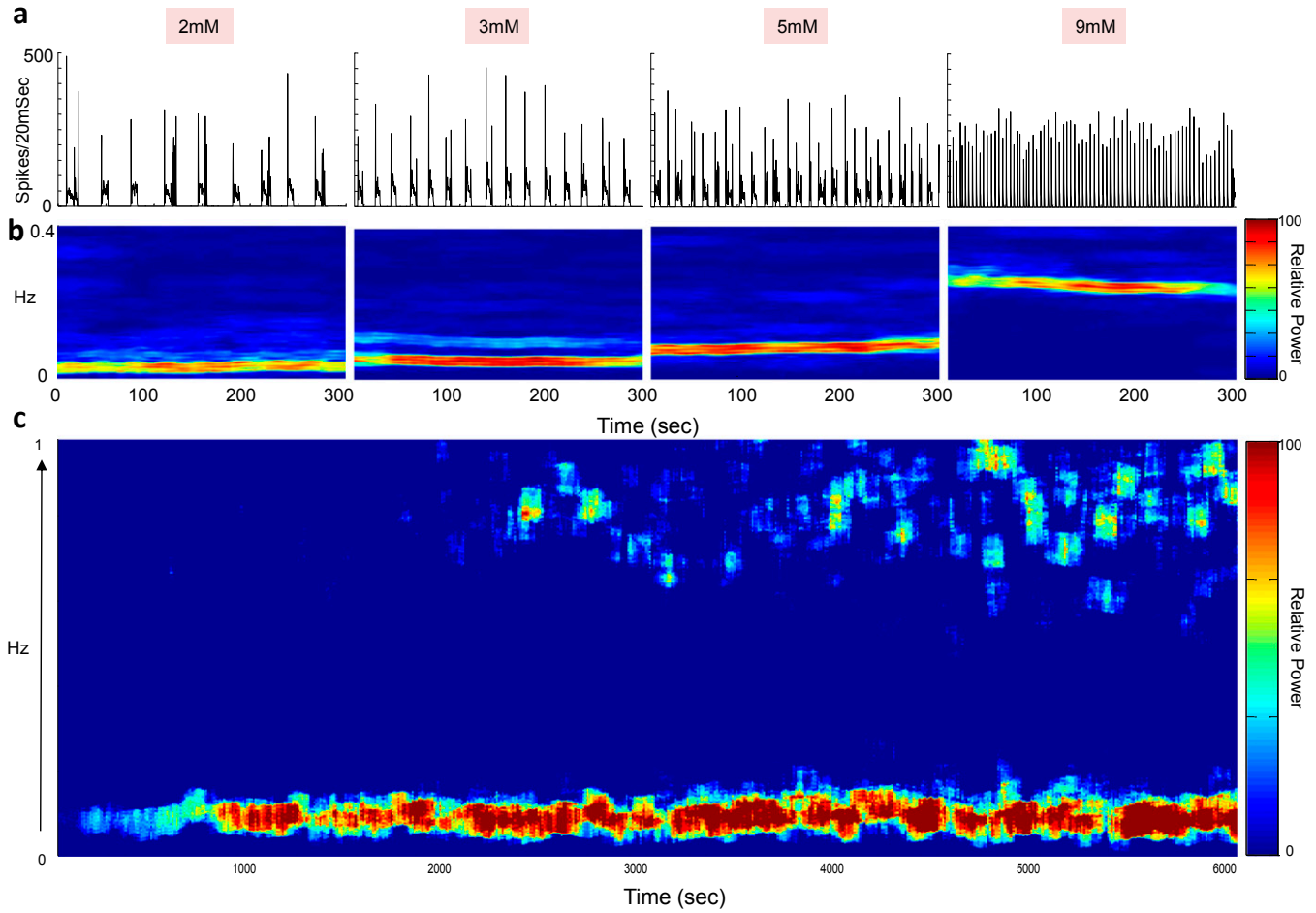

Fig. S1. Stability of network bursts in 1 mM Ca^{2+} medium. (*A*) Network firing rate indicates the appearance of bursts, which increase in frequency as the potassium concentration in the medium is increased from 2 to 9 mM. The increased potassium concentration elevates the resting membrane potential, and is associated with an increase in neuronal excitability. (*B*) Shown are windows of 300 s. FFT spectrograms, calculated over consecutive overlapping windows of 1 min, depict the spectrum of the network activity in *A* as a function of time. (*C*) Example of long-term stability over 6,000 s under constant conditions of 5 mM potassium and 1 mM Ca^{2+}.

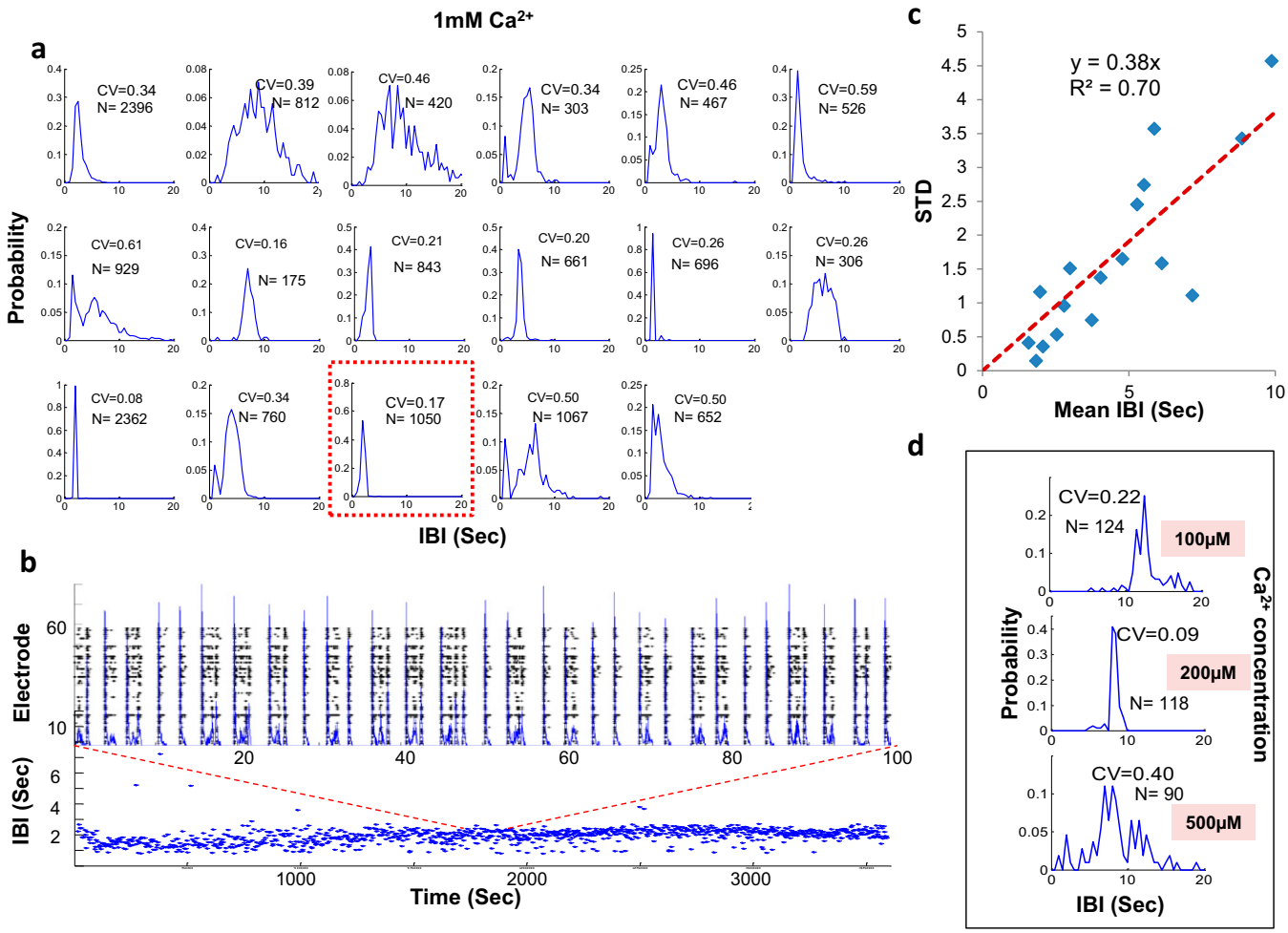

Fig. S2. IBI stability in 1 mM Ca^{2+} medium. (*A*) IBI histograms of 17 cultures, each recorded by a MEA at 1 mM Ca^{2+}. The red outlined panel represents an example of the experiment shown below. (*B*, *Lower*) One hour of the measured IBI plotted by time. (*B*, *Upper*) Zoom-in view showing the neuronal activity in the form of a raster plot (black) and total network firing rate (blue overlay) to demonstrate the appearance of bursts. (*C*) Summary of all experiments shown in *A*. The CV appears to be fixed at CV ~ 0.4 and to be insensitive to the actual IBI. (*D*) IBI histograms at lower Ca^{2+} concentrations.

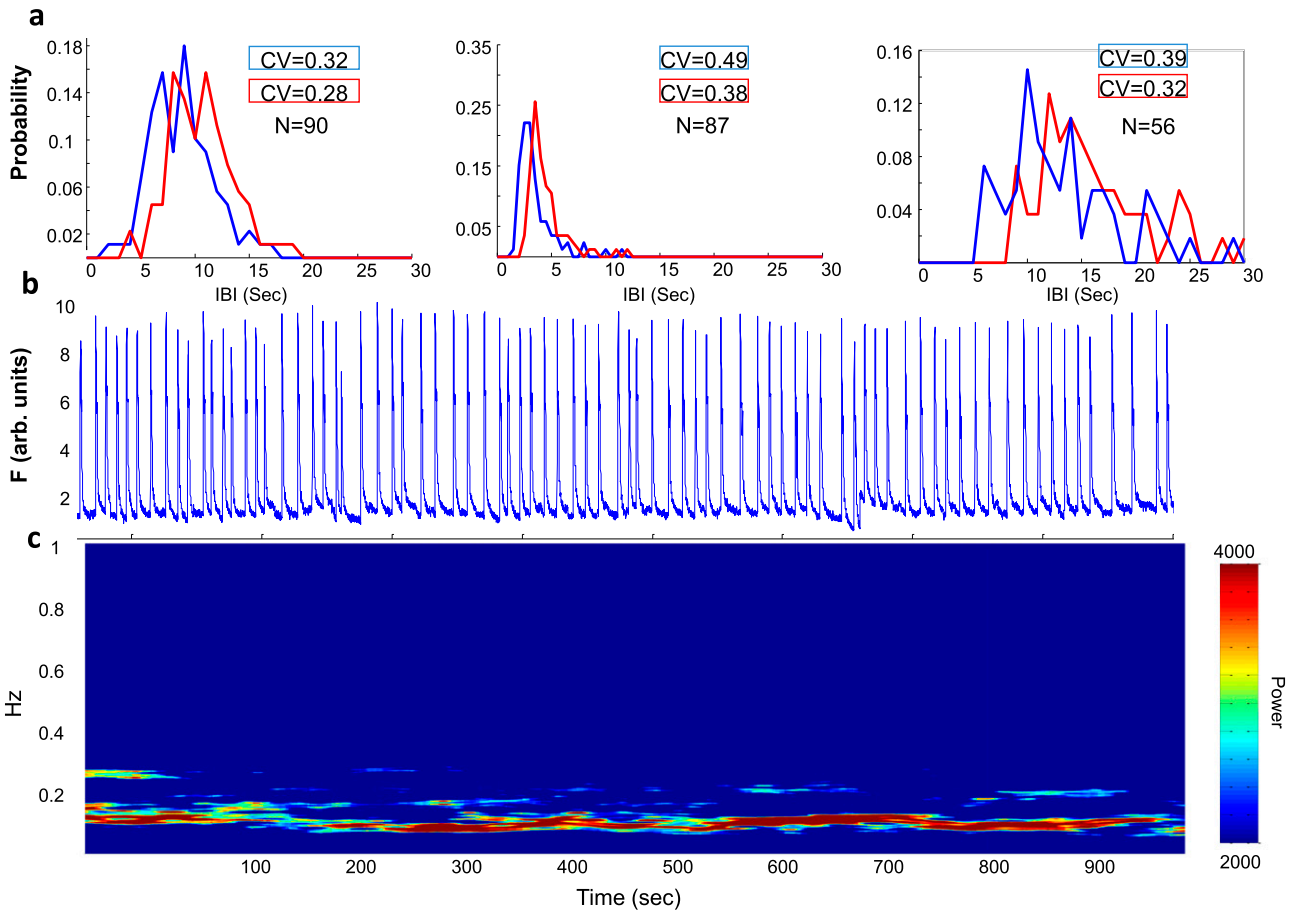

Fig. S3. IBI stability in 1 mM Ca^{2+} medium measured by calcium imaging. (*A*) IBI histograms of three cultures, each recorded at 1 mM Ca^{2+} at room temperature. IBIs were measured either as the interval between the end of one burst and the start of next burst (blue) or from start of one burst to the start of the following burst (red). Representative calcium-imaging fluorescent activity (*B*) and its equivalent spectral analysis (*C*). arb. arbitrary.

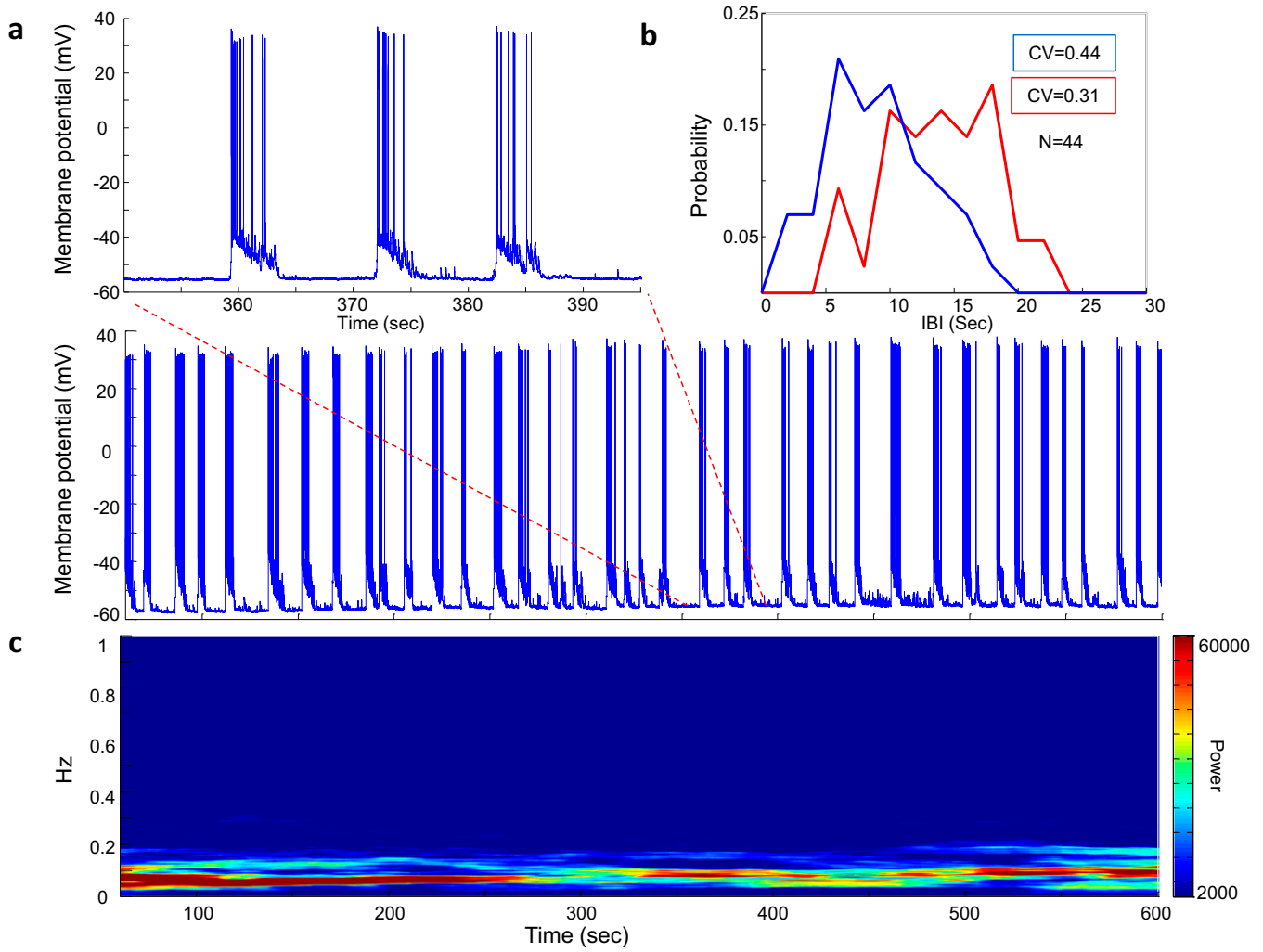

Fig. S4. IBI stability in 1 mM Ca^{2+} medium measured by whole-cell patch clamp. (*A*, *Lower*) Ten minutes of membrane potential activity recorded by patch clamp at room temperature. (*A*, *Upper*) Forty-second zoom-in view of the voltage trace. (*B*) IBIs were measured either as the interval between the end of one burst and the start of next burst (blue) or from start of one burst to the start of the following burst (red). (*C*) Spectral analysis of the fluorescent trace shown above in *A*.

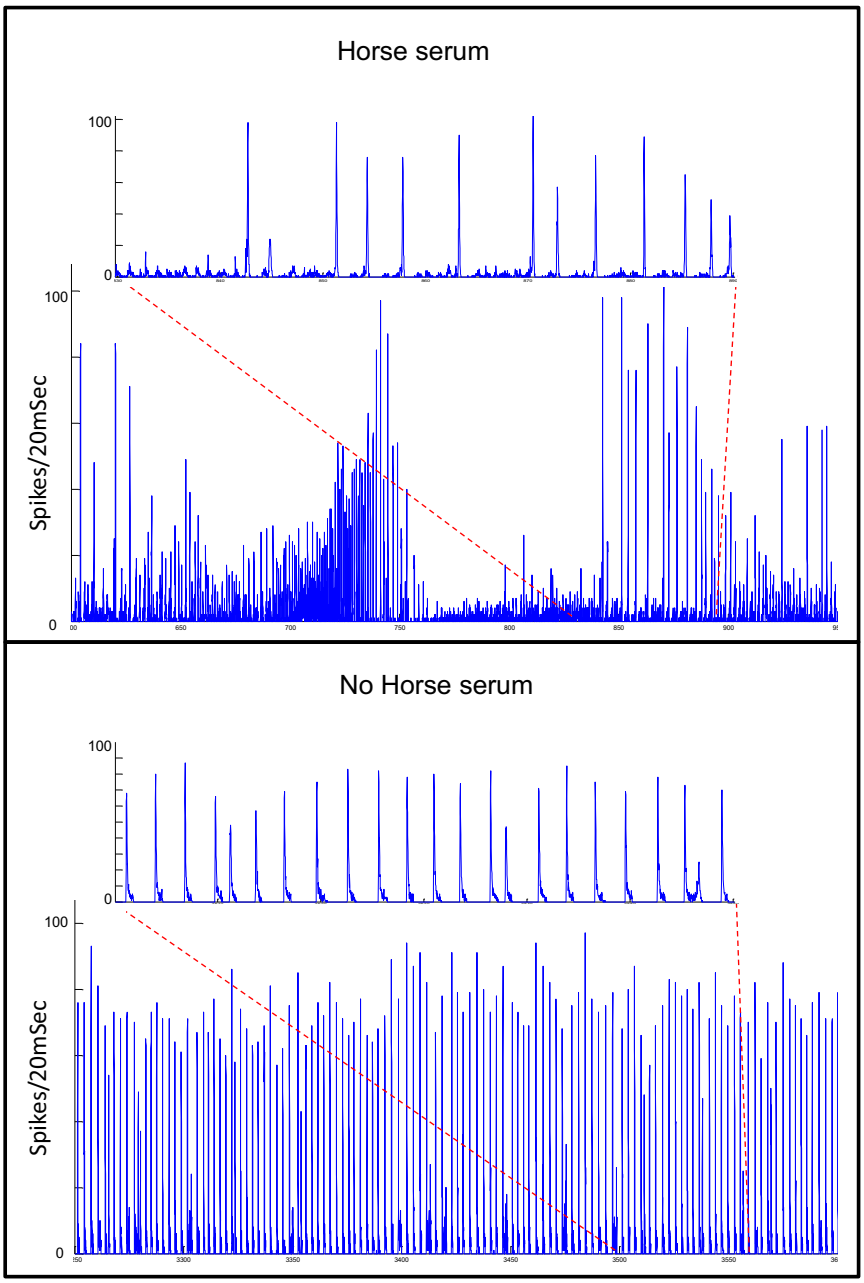

Fig. S5. Horse serum (HS) has a strong impact on network dynamics stability. Three hundred fifty seconds of ongoing network activity were recorded with (*Upper*) and without (*Lower*) the addition of 10% (vol/vol) HS, both under 1 mM extracellular concentration of Ca^{2+}. All other medium components (i.e., ionic composition) were the same. Zoom-in view of 60 s is shown in each condition. Although network activity without HS (*Lower*) is stable and periodic, in the presence of HS (*Upper*), the network behavior becomes irregular with no obviously dominant dynamics. Focus on the individual bursts (zoom-in view) reveals condition-dependent differences in the emergent dynamics and in the overall shape and size of the bursts.

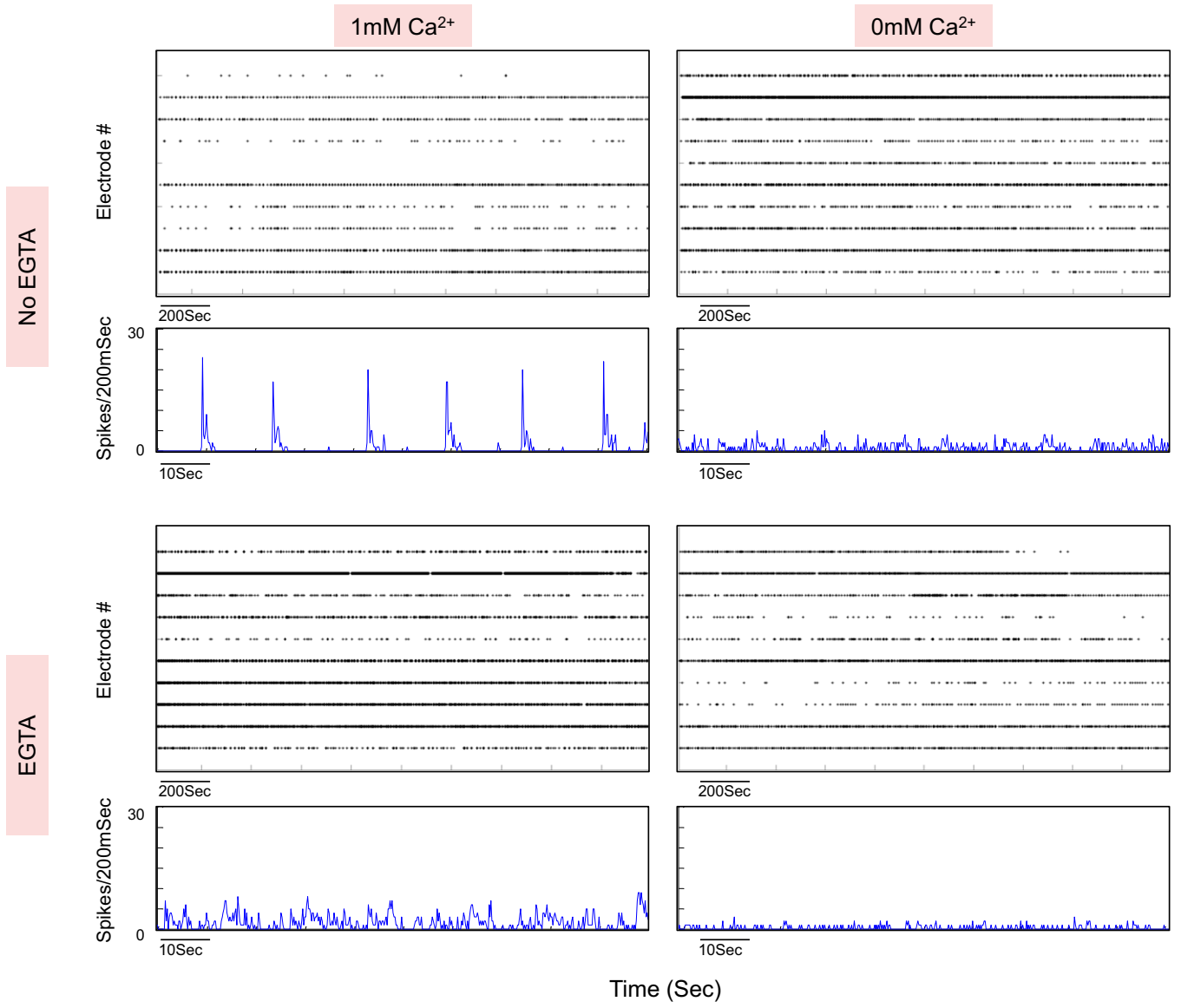

Fig. S6. Control for 0 mM Ca^{2+}. Addition of the Ca^{2+} chelator EGTA to the extracellular medium containing 1 mM Ca^{2+} is similar to changing the extracellular concentration of Ca^{2+} to 0 mM. (*Left*) EGTA eliminated the synchronization between the neurons with little change to the individual neuron's mean firing rate. (*Right*) Likewise, the addition of EGTA to a calcium-free medium had no additional effect.

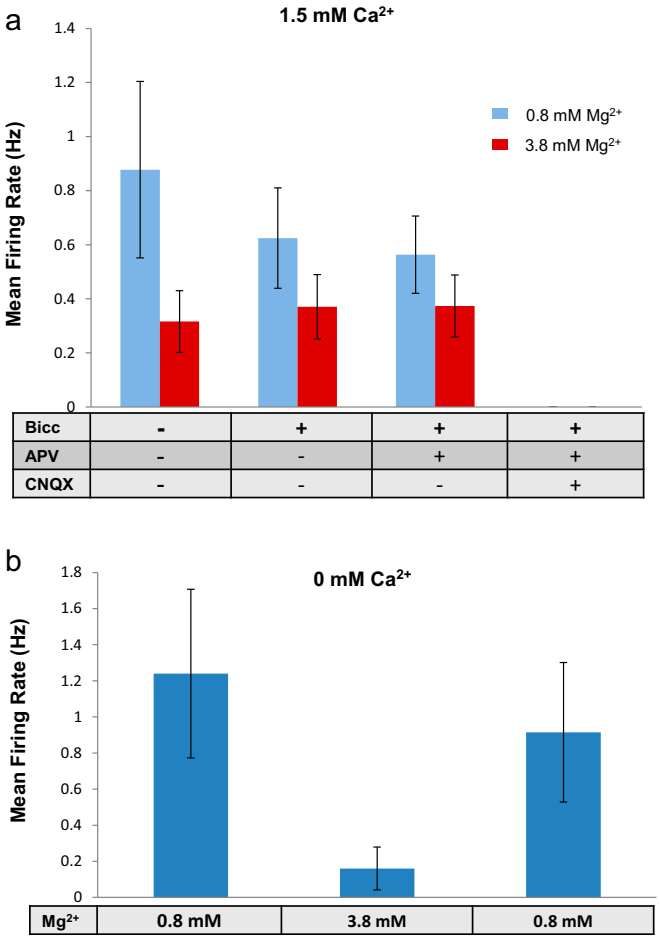

Fig. S7. Synapse-independent effect of elevated extracellular Mg^{2+} on single neuron firing rate. (*A*) Divalent ion magnesium (3 mM) was added to a medium containing the physiological magnesium concentration (0.8 mM) in the presence of 1.5 mM Ca^{2+}. A high magnesium concentration considerably reduced the firing rate. Synaptic blockers were then added to control for a specific magnesium effect stemming from increased blockage of NMDA receptors. Indeed, addition of GABA and NMDA blockers in the presence of high magnesium had no further effect on the mean firing rate of single neurons. As shown in Fig. 1, complete synaptic blockage in the presence of 1.5 mM Ca^{2+} eliminated all activity. (*B*) Similar effect of magnesium was also found at a 0 mM extracellular concentration of Ca^{2+}.

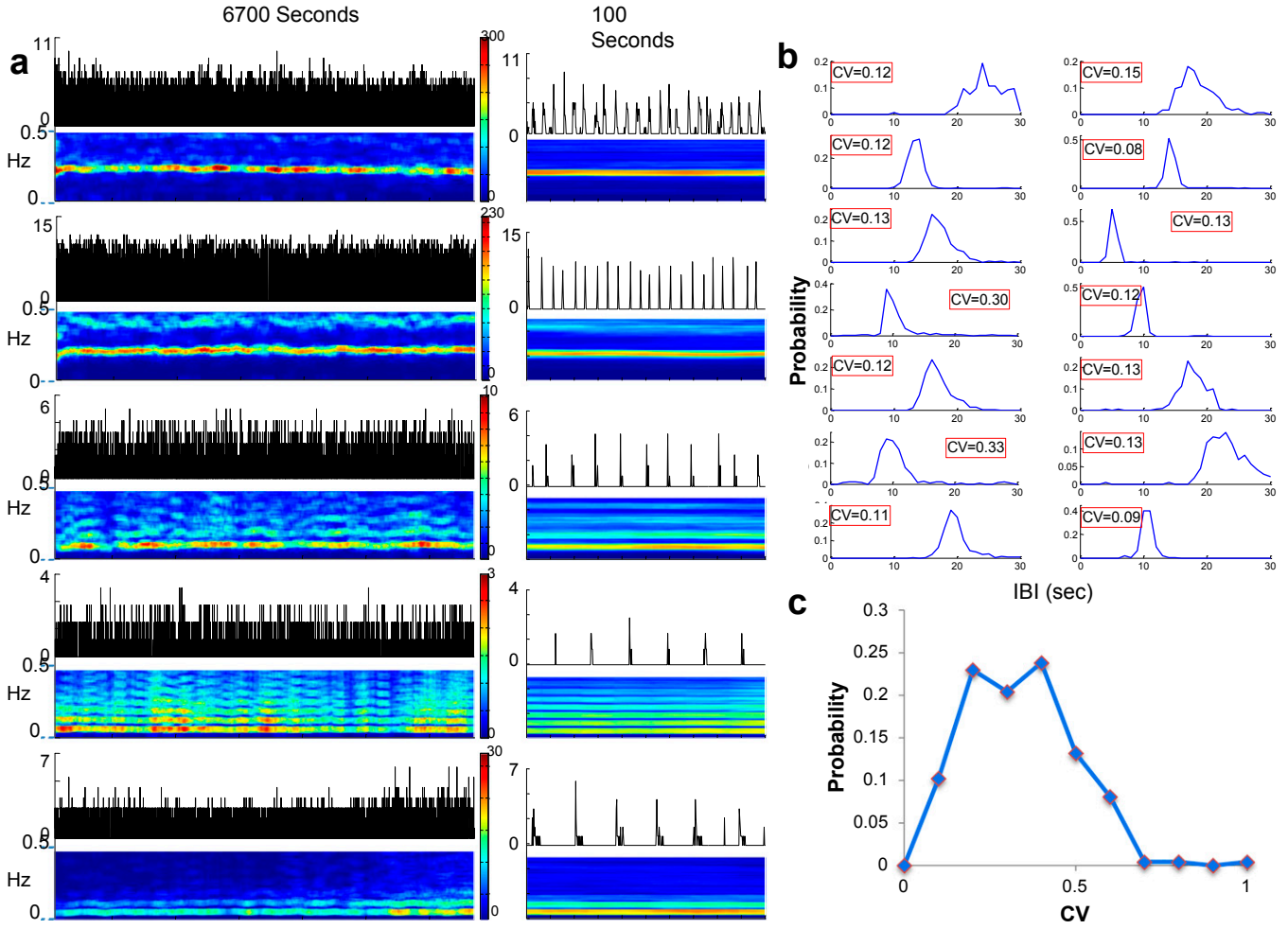

Fig. S8. Stability of individual neuron oscillations in a calcium-free medium. (*A*) Five examples of oscillating neurons are shown, taken from the same culture. The long-term stability measured over about 110 min (*Left*) and a zoom-in view over 100 s (*Right*) are shown. The firing rate (black, spikes per 200 ms) of the individual neuron (*Upper*) with its corresponding FFT spectrogram (*Lower*), taken in overlapping windows of 60 s, are shown. (*B*) IBI histograms and CVs of 14 oscillating neurons. (*C*) Histogram of all individual oscillator CVs.

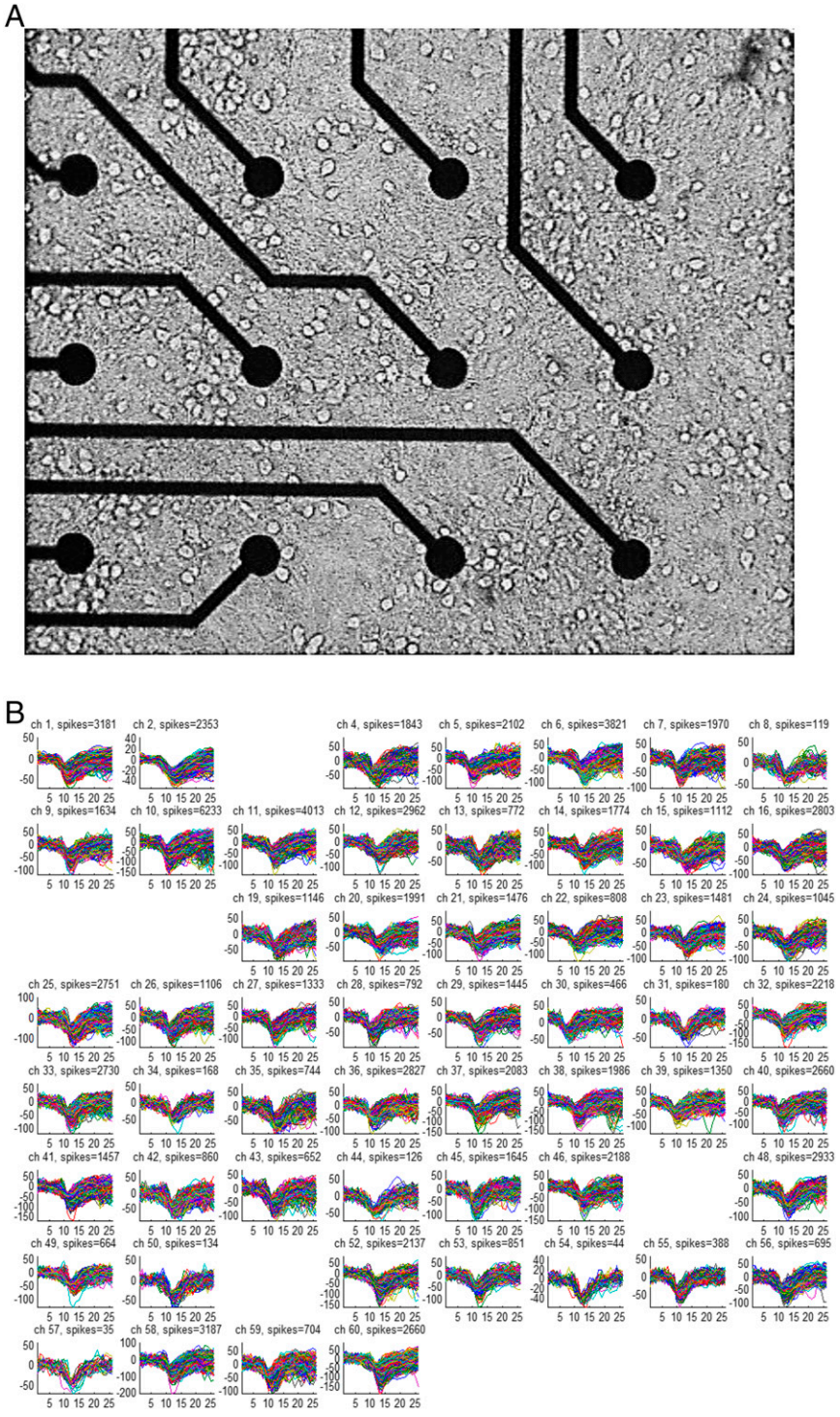

Fig. S9. Multielectrode recording of hippocampal culture. (*A*) Microscope image of 12 of 60 electrodes in 14 DIV hippocampal culture. The spacing between electrodes is 200 μm, and each electrode is 30 μm in diameter. (*B*) Overlay of all spike waveforms detected during a measurement of 1,800 s in each of the 55 active electrodes in this MEA. All electrode amplifier channels (ch) were recorded simultaneously, and the ongoing spike detection was based on the signal-to-noise ratio measured at each of the electrodes separately. The sampling rate was 13 kHz, and the *x* axes are given in units of the sampling points, showing a total of 26 sampling points, equivalent to 1 ms before and 1 ms after spike detection. The *y* axes are given in microvolts.

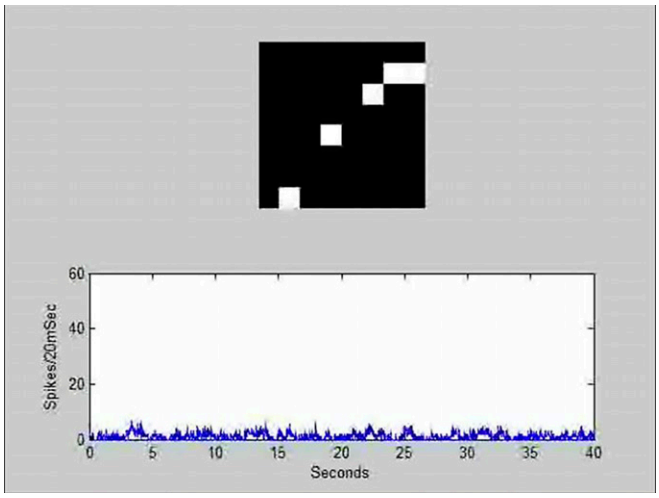

Movie S1. Disconnected network: 0 mM $[Ca^{2+}]_o$. (*Upper*) Relative topography (on the MEA) of the active electrodes. When a neuron fires a spike, its corresponding location flashes in white. (*Lower*) Equivalent total activity (sum of spikes over all electrodes) is shown in 20-ms bins. The same culture (depicted in Fig. 3*A*) is shown in consecutive recordings at different calcium concentrations corresponding to different coupling strengths.

Movie S1

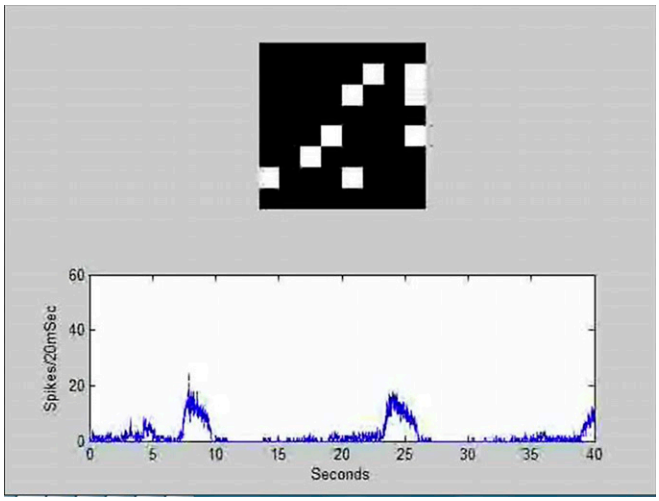

Movie S2. Weakly coupled network: 0.1 mM $[Ca^{2+}]_o$. (*Upper*) Relative topography (on the MEA) of the active electrodes. When a neuron fires a spike, its corresponding location flashes in white. (*Lower*) Equivalent total activity (sum of spikes over all electrodes) is shown in 20-ms bins. The same culture (depicted in Fig. 3*A*) is shown in consecutive recordings at different calcium concentrations corresponding to different coupling strengths.

Movie S2

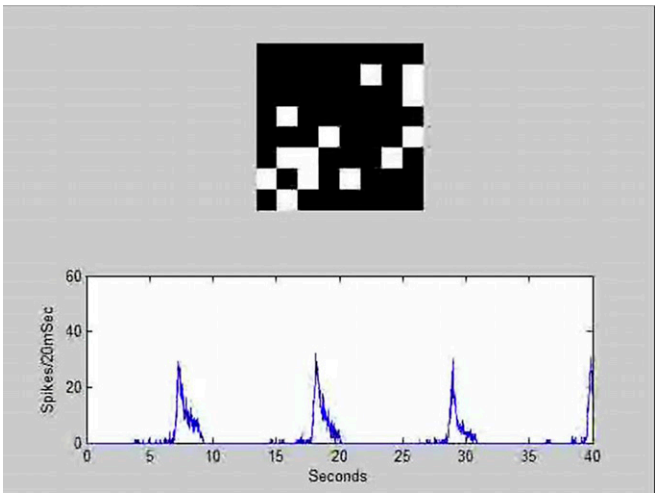

Movie S3. Medium coupled network: 0.2 mM $[Ca^{2+}]_o$. (*Upper*) Relative topography (on the MEA) of the active electrodes. When a neuron fires a spike, its corresponding location flashes in white. (*Lower*) Equivalent total activity (sum of spikes over all electrodes) is shown in 20-ms bins. The same culture (depicted in Fig. 3*A*) is shown in consecutive recordings at different calcium concentrations corresponding to different coupling strengths.

Movie S3

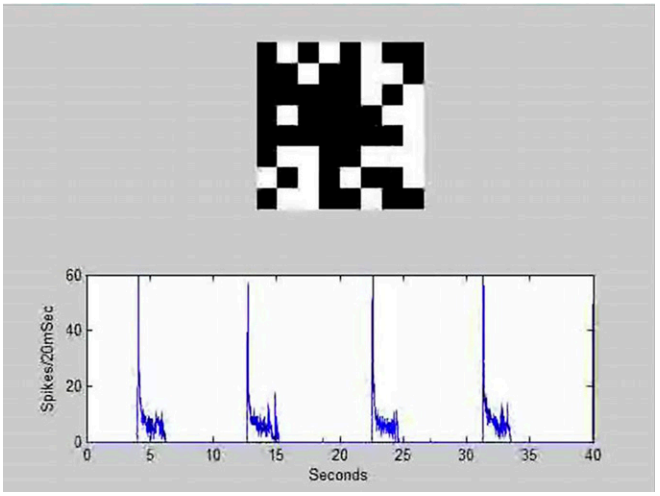

Movie S4. Strongly coupled network: 0.5 mM $[Ca^{2+}]_o$. (*Upper*) Relative topography (on the MEA) of the active electrodes. When a neuron fires a spike, its corresponding location flashes in white. (*Lower*) Equivalent total activity (sum of spikes over all electrodes) is shown in 20-ms bins. The same culture (depicted in Fig. 3*A*) is shown in consecutive recordings at different calcium concentrations corresponding to different coupling strengths.

Movie S4